Journal of Organometallic Chemistry 901 (2019) 120945

Contents lists available at ScienceDirect

Journal of Organometallic Chemistry

journal homepage: www.elsevier.com/locate/jorganchem

Methane generation via intraprotein C–S bond cleavage in cytochrome b_{562} reconstituted with nickel didehydrocorrin

Yuta Miyazaki [a], Koji Oohora [a, b, *], Takashi Hayashi [a, **]

[a] Department of Applied Chemistry, Graduate School of Engineering, Osaka University, Suita, 565-0871, Japan
[b] Frontier Research Base for Global Young Researchers, Graduate School of Engineering, Osaka University, Suita, 565-0871, Japan

ARTICLE INFO

Article history:
Received 20 August 2019
Received in revised form
16 September 2019
Accepted 18 September 2019
Available online 19 September 2019

Keywords:
Hemoprotein
MCR
F430
Methane
Nickel corrinoid

ABSTRACT

Cytochrome b_{562} (Cyt b_{562}) reconstituted with nickel didehydrocorrin (Ni^{II}(DDHC)), a protein-based functional model of methyl-coenzyme M reductase (MCR), was investigated to demonstrate methane generation via intraprotein cleavage of a C–S bond. Ni^{II}(DDHC) was synthesized as a model complex of an MCR cofactor known as F430 and found to show Ni^{II}/Ni^{I} redox behavior with a potential of −0.61 V vs. Ag|AgCl. This potential is slightly positive-shifted compared to that of F430 without protein. Conjugation of Ni^{II}(DDHC) with the apo-form of Cyt b_{562} provides reconstituted Cyt b_{562} (rCyt b_{562}(Ni^{II}(DDHC))) which was characterized by spectroscopic measurements. Photoirradiation of rCyt b_{562}(Ni^{II}(DDHC)) generates methane gas in the presence of tris(2,2′-bipyridine)ruthenium(II) chloride as a photosensitizer and sodium ascorbate as a sacrificial reagent. Further experiments using Cyt b_{562} mutants indicate that methane is derived from the CH_3S group of the methionine residue in the heme-binding site where thioether, thiol and the nickel center are precisely arranged. The present study demonstrates the first example of methane generation via intraprotein cleavage of a C–S bond using a functional model of MCR.

1. Introduction

Methane has been investigated both as an alternative fuel and a greenhouse gas. Most of the methane gas in nature is generated as an end-product of decomposition of organic compounds by archaea under anaerobic conditions [1,2]. Methanogenic archaea are known to possess the enzyme methyl-coenzyme M reductase (MCR) which catalyzes the final and rate-limiting step of biological methane generation [3–5]. This reaction is promoted by a nickel hydrocorphinoid cofactor known as F430 in the active site. Methyl-coenzyme M (CH_3S–CoM) and coenzyme B (HS–CoB) are converted to methane and the heterodisulfide compound (CoM–S–S–CoB) by the active Ni(I) intermediate in the enzymatic reaction (Fig. 1).

In spite of investigations in various experimental and theoretical studies, the reaction mechanism of MCR has not yet been fully elucidated because of the complicated structure of MCR [6–27]. At this moment, two plausible mechanisms have been proposed which include formation of an organometallic methyl–Ni(III) intermediate or a methyl radical intermediate [5]. In the former case, the stable methyl–Ni(III) intermediate is detected in a reaction of the active Ni(I) species of MCR with methyl iodide [13–17]. The latter mechanism is more plausible according to a recent study which included a detailed analysis of single turnover reaction of MCR with substrates possessing the CH_3S group, which are similar to native substrates [22]. In this context, an appropriate model complex of F430 has been required to properly assess the physicochemical properties and reactivity of F430 [28–32]. Although some model complexes generate methane from activated methyl donors, examples of methane generation via cleavage of a C–S bond have been quite limited. Jaun and co-workers reported that photoirradiation of a Ni(II) complex with a thiolate-thioether ligand, bis{1-[2-(methylthio)ethyl]cyclohexanethiolato}nickel, in the presence of the corresponding thiol-thioether substrate, 1-[2-(methylthio)ethyl]cyclohexanethiol, generated methane gas and the disulfide 1,2-dithiaspiro[4.5]decane, via cleavage of the C–S bond [30]. Tatsumi and co-workers also reported that chemical reduction of Ni(II) complexes with thioether ligands, 1,8-dimethyl-4,11-bis{(2-methylthio)ethyl}-1,4,8,11-tetraaza-1,4,8,11-cyclotetradecane and 1,8-{bis(2-methylthio)ethyl}-1,4,8,11-

* Corresponding author. Department of Applied Chemistry, Graduate School of Engineering, Osaka University, Suita, 565-0871, Japan.
** Corresponding author.
E-mail addresses: oohora@chem.eng.osaka-u.ac.jp (K. Oohora), thayashi@chem.eng.osaka-u.ac.jp (T. Hayashi).

https://doi.org/10.1016/j.jorganchem.2019.120945
0022-328X/

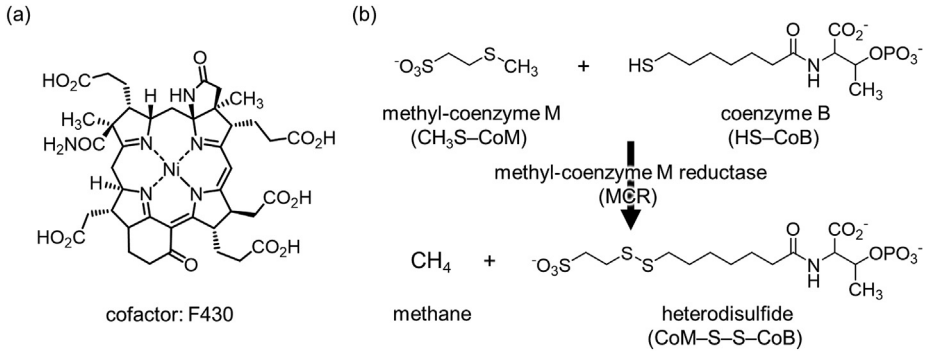

Fig. 1. (a) Molecular structure of cofactor F430. (b) Methane generation catalyzed by methyl-coenzyme M reductase (MCR) in methanogenic archaea.

tetraaza-1,4,8,11-cyclotetradecane, generates methane and ethane gases via intramolecular cleavage of the C—S bond. The further addition of a thiol compound, 2,6-dimesitylbenzenethiol, promotes methane generation [31]. These model systems mimicking the enzymatic reaction have provided important insights into our understanding of the reaction mechanism of MCR.

In our previous work, we have reported a protein-based functional MCR model which is prepared by myoglobin reconstituted with nickel tetradehydrocorrin (Ni(TDHC)) as a model complex of F430 [33]. The active Ni(I) species was confirmed in the presence and absence of the protein matrix of myoglobin. The protein-based functional model was found to promote methane gas generation from methyl iodide, whereas the bare Ni(TDHC) complex does not generate any significant amounts of methane gas under the same condition, indicating the importance of a protein matrix. However, even the Ni(I) species of Ni(TDHC) in the protein matrix of myoglobin appears to be insufficient to activate a substrate involving a CH_3S group as seen in catalysis by MCR. Thus, to enhance the reactivity of the Ni(I) species, we have recently constructed a different type of protein-based functional model of MCR by conjugation of nickel didehydrocorrin (Ni(DDHC)) and the apoform of cytochrome b_{562} (Cyt b_{562}) in an effort to replicate methane generation via C—S bond cleavage (Fig. 2). This is because the Ni(I) species of Ni(DDHC) is expected to be a more reactive intermediate than the Ni(I) species of Ni(TDHC). Previous investigations have found that the nucleophilicity of the Co(I) species of cobalt didehydrocorrin (Co(DDHC)) is enhanced relative to the Co(I) species of cobalt tetradehydrocorrin (Co(TDHC)) [34,35]. In addition, Cyt b_{562} is a suitable protein matrix because the CH_3S group of the methionine residue, Met7, is located close to the metal center in the heme pocket. In this paper, methane generation by present functional model via intraprotein cleavage of the C—S bond of Met7 upon photoreduction of the nickel complex is demonstrated in reconstituted Cyt b_{562} as shown in Fig. 2.

2. Experimental

2.1. Instruments

UV—vis spectral measurements were carried out with a BioSpec-nano spectrophotometer (Shimadzu) or a V-670 spectrophotometer (JASCO). CD spectra were recorded on a J-820AC spectropolarimeter (JASCO). ESI-TOF MS analyses were performed with a micrOTOF-II mass spectrometer (Bruker). ^{1}H NMR spectrum was collected on an Avance III (600 MHz) spectrometer (Bruker). The ^{1}H NMR chemical shift values are reported in ppm relative to a

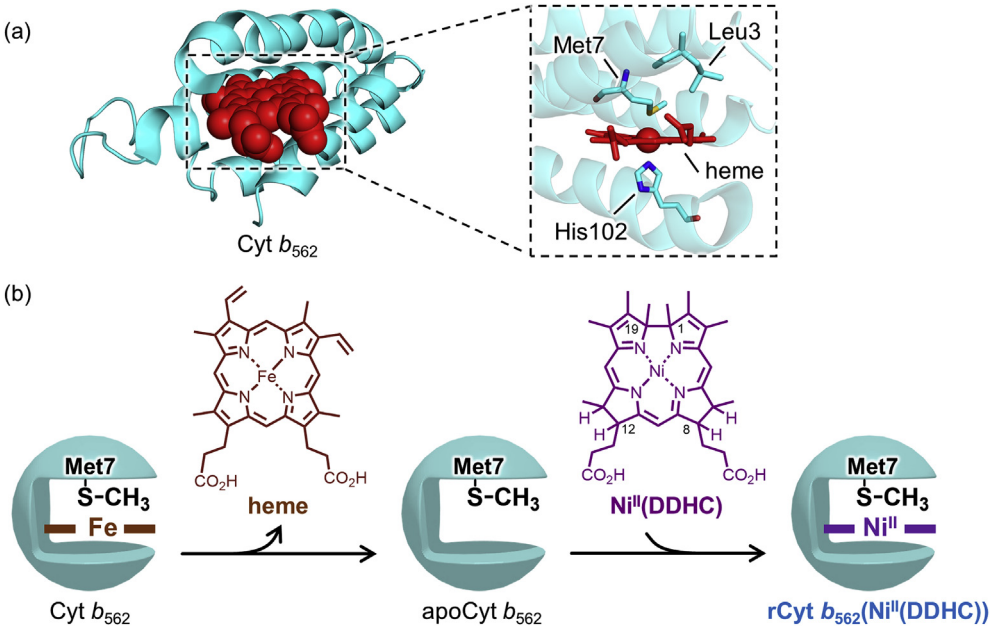

Fig. 2. (a) Structure of Cyt b_{562} (PDB ID: 1QPU). (b) Schematic representation of the reconstitution of Cyt b_{562} with Ni(DDHC).

residual solvent peak. ICP-OES was performed on an ICPS-7510 emission spectrometer (Shimadzu). Electrochemical studies were performed using a potentiostat (CompactStat, Ivium Technologies). A single-compartment cell was used for all cyclic voltammetry (CV) experiments with a polished Pt working electrode, a Pt wire counter electrode and an Ag|AgCl (3 M NaCl) reference electrode (ALS Co., Ltd.). All electrochemical experiments were performed with 100 mM tetrabutylammonium hexafluorophosphate ($TBAPF_6$) as a supporting electrolyte. All solutions were purged with N_2 before CV measurements. Air-sensitive manipulations were performed in a UNILab glove box (MBRAUN). Purification by HPLC was conducted with a HPLC Prominence System (Shimadzu). Size exclusion chromatographic (SEC) purification was performed using an ÄKTApurifier system (GE Healthcare). The pH measurements were made with an F-72 pH meter (Horiba). Photoirradiation reaction was conducted using an Optical Modulex (USHIO Inc.) equipped with a 500 W Xe arc lamp, a cold filter (Asahi Spectra Co., Ltd.) and a 420 nm sharp cut filter (SIGMAKOKI Co., Ltd.) to produce light in the range of $420 \leq \lambda \leq 750$ nm for 2 h at 25 °C in a cryostat (CoolSpeK, UNISOKU Co., Ltd.) under an N_2 atmosphere. Methane gas was quantified by gas chromatography, GC-2010 plus (Shimadzu) equipped with a BID detector.

2.2. Materials

All reagents of the highest guaranteed grade available were obtained from commercial sources and were used as received unless otherwise indicated. A standard nickel solution for ICP-OES was purchased from FUJIFILM Wako Pure Chemical Corporation. $TBAPF_6$ (>98% purity) was purchased from Tokyo Chemical Industry Co., Ltd., and recrystallized from heated ethanol and dried under vacuum before use. Authentic methane gas (0.408% (*v*/*v*), balancer: Ar) was purchased from GL Sciences Inc. Distilled water was demineralized using a Millipore Integral 3 apparatus. Nickel tetradehydrocorrin (Ni(TDHC)) was prepared according to the previous report [33]. Apo-forms of Cyt b_{562} and Cyt $b_{562}{}^{M7L}$ were prepared by acidification followed by extraction of heme with 2-butanone (Teale's conventional method) [36]. Apo-form of Cyt $b_{562}{}^{L3C}$ was prepared by dialysis against 50 mM potassium phosphate buffer (pH 7.0) containing 0.1% sodium dodecyl sulfate and 1% 2-mercaptoethanol at 30 °C for 20 h followed by further dialysis against 100 mM potassium phosphate buffer (pH 7.0) as reported in the literature [37].

2.3. Synthesis of nickel (II) didehydrocorrin (Ni^{II}(DDHC))

In a two-necked flask, 10% palladium on carbon (24 mg) was added into a solution of Ni^{II}(TDHC) (20 mg, 28 μmol) in methanol (8 mL) containing 1% (*v*/*v*) acetic acid and hydrogenation was performed under 0.1 MPa of H_2 atmosphere at 65 °C for 3.5 h. The reaction solution was filtered and evaporated under reduced pressure. After the residue was dissolved in dichloromethane (50 mL), the solution was washed with brine (30 mL) and water (30 mL) for three times and dried with Na_2SO_4. This crude product was purified by reverse phase HPLC (acetonitrile/H_2O eluent, C18 column). The desired fraction was collected and evaporated under reduced pressure. After evaporation, Ni^{II}(DDHC) (17.6 mg, 88% yield) was obtained as yellow powder. Although the ^1H NMR spectrum of purified Ni^{II}(DDHC) in CD_2Cl_2 was measured, each peak is difficult to be assigned because of the existence of two diastereomers and their conformers (Figs. S1 and S2). HRMS (ESI, positive mode, *m*/*z*): $[M - ClO_4]^+$ calcd. for $C_{33}H_{41}N_4O_4Ni$, 615.2476; found, 615.2478. UV–Vis (H_2O, (nm) ε ($M^{-1}\cdot cm^{-1}$)): $\lambda_{max} = 264$ (20800), 295 (22800), 321 (21500), 453 (11400).

2.4. Protein sequence of Cyt b_{562} and its mutants

2.4.1. Cyt b_{562}

ADLEDNMETLNDNLKVIEKADNAAQVKDALTKMRAAALDAQKATP
PKLEDKSPDSPEMKDFRHGFDILVGQIDDALKLANEGKVKEAQAAAEQ
LKTTRNAYHQKYR

2.4.2. Cyt $b_{562}{}^{M7L}$

ADLEDNLETLNDNLKVIEKADNAAQVKDALTKMRAAALDAQKATPP
KLEDKSPDSPEMKDFRHGFDILVGQIDDALKLANEGKVKEAQAAAEQLK
TTRNAYHQKYR

2.4.3. Cyt $b_{562}{}^{L3C}$

ADCEDNMETLNDNLKVIEKADNAAQVKDALTKMRAAALDAQKATP
PKLEDKSPDSPEMKDFRHGFDILVGQIDDALKLANEGKVKEAQAAAEQL
KTTRNAYHQKYR

2.5. Expression and purification of Cyt b_{562} and its mutants

The gene expression systems used to obtain wild type Cyt b_{562} was reported in our previous paper [38]. Site-directed mutagenesis was performed by the polymerase chain reaction (PCR) using the KOD-Plus-Neo kit (Toyobo Life Science) according to the protocol of the manufacturer. The wild type Cyt b_{562} gene cloned into pUC118 was used as a template to introduce M7L and L3C single mutation into the Cyt b_{562} matrix. The primer sequences used to generate each mutant were:

M7L: (5′-CGTTTGCCGCTGATCTTGAAGACAATCTGGAAACCCTCA ACGAC-3′) and the complementary primer;

L3C: (5′-CTGCGTCGTTTGCCGCTGATTGCGAAGACAATATGGAAA CCCTC-3′) and the complementary primer.

After PCR, the template DNA plasmids were digested with Dpn I (Thermo Fisher Scientific). *E. coli* DH5α competent cells were transformed with the PCR products. After the cultivation, the plasmids were purified using the NucleoSpin Plasmid EasyPure (Takara). DNA sequencing was performed to verify each correct mutation in the gene sequence. The resulting expression plasmid was used to transform *E. coli* strain TG1. YT medium (6 L) containing ampicillin (600 mg) was inoculated with 150 mL of the culture (OD = 0.5) of the transformed cells. After the cells were grown aerobically with vigorous shaking at 37 °C for 12 h, the cells were harvested by centrifugation. The harvested cells from 6 L of culture were re-suspended in ca. 100 mL of a 10 mM Tris–HCl buffer (pH 8.0) and lysed by the addition of chloroform (ca. 2 mL). After stirring for 1 h at 4 °C, 10 mM Tris-HCl (pH 8.0) (ca. 200 mL) was added to the lysate. Then, the lysate was stirred for 1 h at 4 °C again and centrifuged to collect supernatant. The pH value of the supernatant was adjusted to 4.5 by the addition of 1 M HCl. After stirring for 1 h at 4 °C, the precipitate was removed by centrifugation. In the case of the M7L mutant, excess amount of hemin (final conc.: ca. 30 μM) was added before acidification by 1 M HCl to convert the apo-form to the holo-form. The supernatant was loaded onto a CM-52 cellulose (FUJIFILM Wako Pure Chemical Corporation) cation-exchange column pre-equilibrated with 50 mM KH_2PO_4 containing 0.1 mM EDTA (pH 4.5). The fraction of the target protein was collected by an eluent gradiented with (A) 50 mM KH_2PO_4 containing 0.1 mM EDTA and 50 mM KCl (pH 4.5) and (B) 50 mM KH_2PO_4 containing 0.1 mM EDTA and 150 mM KCl (pH 4.5). The obtained solution was concentrated using an Amicon stirred cell equipped with a 5 kDa molecular weight cut-off ultrafiltration membrane (Millipore). The concentrated solution was passed through a HiPrep 16/60 Sephacryl S-200 HR column equilibrated with 100 mM potassium phosphate buffer (pH 7.0) using an ÄKTApurifier system (GE Healthcare). The fractions with $R_z > 5$ (R_z

is a ratio of absorbance values at 418 nm and 280 nm) were collected and concentrated. The obtained Cyt b_{562} mutants were characterized by SDS-PAGE and ESI-TOF MS (Fig. S3), and stored at −80 °C.

2.6. Preparation of reconstituted Cyt b_{562} with Ni^{II}(DDHC) or Ni^{II}(TDHC)

To a solution of Ni^{II}(DDHC) or Ni^{II}(TDHC) (final conc.: 50 μM) in 100 mM potassium phosphate buffer (pH 7.0), an apoCyt b_{562} solution (final conc.: 150 μM) in 100 mM potassium phosphate buffer (pH 7.0) was added under an N_2 atmosphere at 25 °C. The obtained reconstituted Cyt b_{562} (rCyt b_{562}(Ni^{II}(DDHC)) or rCyt b_{562}(Ni^{II}(TDHC))) aqueous solution was used for experiments without purification.

2.7. Photo-induced methane generation from reconstituted Cyt b_{562}

In an optical cell (pathlength: 1 mm, volume: 1000 μL) sealed with a silicon septum, a solution of Ni^{II}(DDHC) or Ni^{II}(TDHC) (final conc.: 50 μM), apoCyt b_{562} (final conc.: 150 μM), tris(2,2′-bipyridine) ruthenium(II) chloride (final conc.: 100 μM), sodium ascorbate (final conc.: 100 mM) dissolved in 100 mM potassium phosphate buffer (pH 7.0) (100 μL in total volume) was prepared. The solution was then irradiated using an Optical Modulex (USHIO Inc.) equipped with a Xe lamp and optical filters to produce visible light for 2 h at 25 °C under an N_2 atmosphere. After photoirradiation, the gas sample (100 μL) was carefully taken from the headspace of the vial by a gastight syringe and injected into a GC-2010 plus (Shimadzu) equipped with a BID detector and a 2.0 m × 1.0 mm ID micropacked column SHINCARBON-ST 80–100 mesh using He as a carrier gas. Measurement conditions: injector temperature = 200 °C, split ratio 5:1, detector temperature = 250 °C, column temperature = 60 °C (1 min hold) − 18 °C/min − 220 °C (2 min hold), column flow rate 55.8 mL/min. The product was identified by a comparison of its retention time with that of the authentic standard sample. The amount of methane gas was determined from the area of the corresponding eluted peak using the calibration curve.

2.8. Mass spectral analysis of the protein matrix after the photoirradiation reaction

Protein matrices in reaction solutions (200 μL) were purified using a HiTrap Desalting column (5 mL, GE Healthcare) with 50 mM ammonium acetate buffer under aerobic conditions. The obtained protein solutions were concentrated using an Amicon Ultra 0.5 mL Centrifugal Filter with a 3-kDa molecular weight cut-off membrane (Millipore). The concentrated protein solutions (50 μL) were mixed with 0.1% formic acid in methanol (50 μL) and analyzed by a micrOTOF-II mass spectrometer (Bruker).

3. Results and discussion

We designed a Ni(DDHC) cofactor having a monoanionic tetrapyrrole ligand and two propionate side chains at the C8- and C12-positions for the purpose of fixing the cofactor in the proper position via a hydrogen bonding network with polar amino acid residues in the heme binding pocket. Ni^{II}(DDHC) was synthesized by hydrogenation of Ni^{II}(TDHC) with 10% Pd on carbon in methanol containing 1% acetic acid under ambient pressure of H_2 (Scheme 1). The ESI-TOF mass spectrum of Ni^{II}(DDHC) provides a peak at m/z = 615.2478 with a characteristic isotope pattern of a compound containing nickel ion, which is consistent with the calculated exact

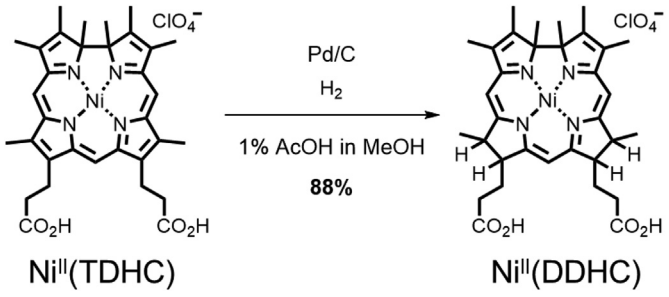

Scheme 1. Synthesis of Ni^{II}(DDHC).

mass number for $[M-ClO_4]^+$ (calcd.: m/z = 615.2476). The UV–vis spectrum provides characteristic peaks at 264, 295, 321 and 453 nm in aqueous solution (Fig. 3). The CV measurements revealed two reversible redox peaks at −0.61 and 0.44 V vs. Ag|AgCl in acetonitrile as shown in Fig. 4. The former redox peak is assigned to the Ni^{II}/Ni^{I} process, which is negatively shifted by 0.16 V compared to that of Ni^{II}(TDHC) (Fig. S4), indicating an increase in the reactivity of the Ni(I) species. The latter redox peak should be attributed to the Ni^{III}/Ni^{II} process, which is not observed in Ni^{II}(TDHC). The redox potentials corresponding to the Ni^{II}/Ni^{I} process at −0.61 V vs. Ag|AgCl and the Ni^{III}/Ni^{II} process at 0.44 V vs. Ag|AgCl are slightly positive-shifted compared to the reported potential data of the pentamethyl ester of F430 (Ni^{II}/Ni^{I}: 0.70 V in dimethylformamide, Ni^{III}/Ni^{II}: 0.43 V in acetonitrile) [6–8].

Next, rCyt b_{562}(Ni^{II}(DDHC)) as a protein-based model of MCR was prepared by conjugation of Ni^{II}(DDHC) with the apo-form of Cyt b_{562} (apoCyt b_{562}) because the hydrophobic cofactor-binding cavity of Cyt b_{562} provides a hexacoordinated structure of the native heme with two axial ligands, His102 and Met7 (Fig. 2) [39], and the CH_3S group of Met7 side chain is expected to work as an intraprotein methyl donor. The UV–vis spectra do not show significant changes upon addition of apoCyt b_{562} to a Ni^{II}(DDHC) aqueous solution (Fig. 5). In contrast, the addition of Ni^{II}(DDHC) to apoCyt b_{562} exhibits stronger CD peaks at 208 and 222 nm derived from α-helices compared to those of apoCyt b_{562}, which support the formation of the reconstituted protein (Fig. 6). In fact, according to previous studies on hemoprotein reconstitutions, the insertion of

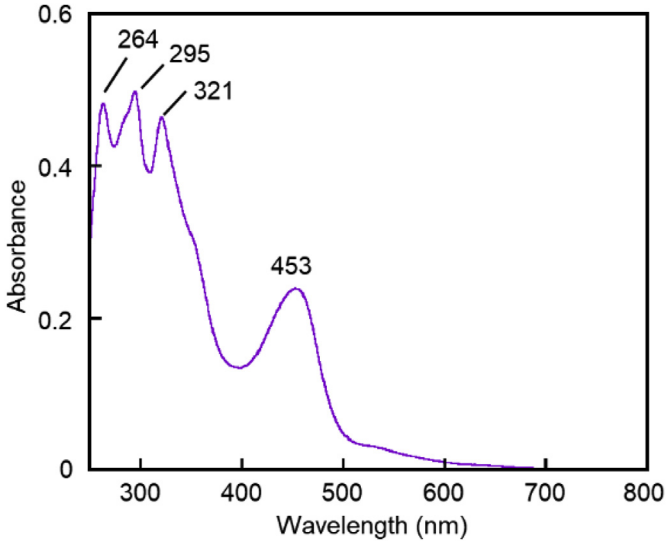

Fig. 3. UV–vis spectrum of Ni^{II}(DDHC) in 100 mM potassium phosphate buffer (pH 7.0) at 25 °C.

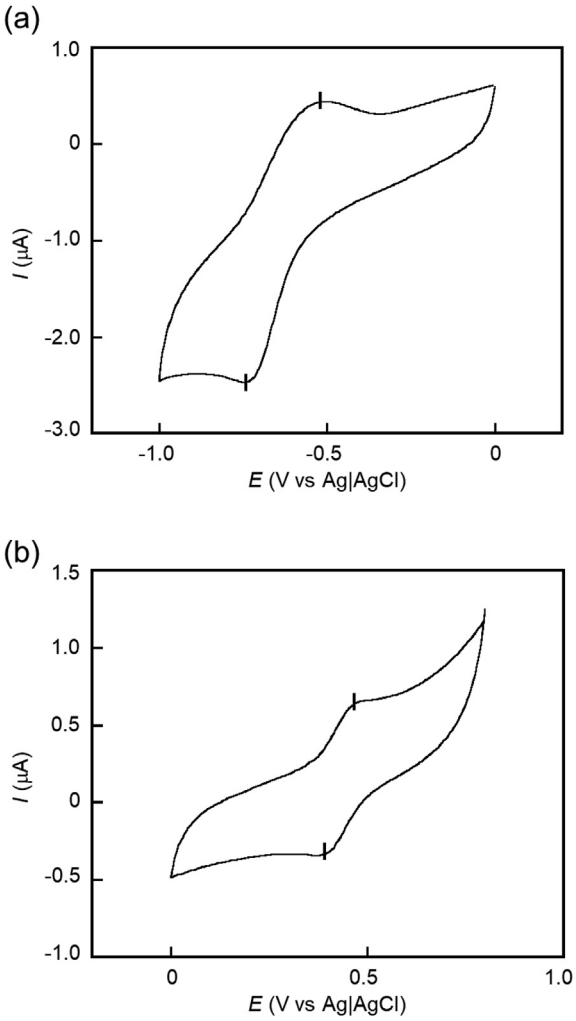

Fig. 4. Cyclic voltammogram of Ni^{II}(DDHC) in anhydrous acetonitrile with 100 mM $TBAPF_6$ with a scan rate of 100 mV/s under an N_2 atmosphere. Sweeping range: (a) −1.0 to 0 V, (b) 0 to 0.8 V.

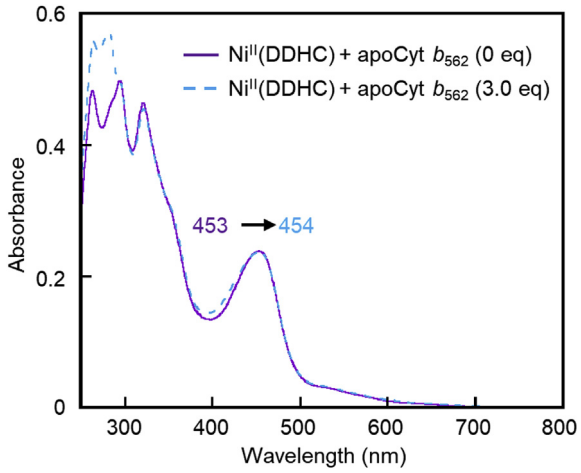

Fig. 5. UV−vis spectral changes of Ni^{II}(DDHC) before and after addition of apoCyt b_{562} in 100 mM potassium phosphate buffer (pH 7.0) at 25 °C.

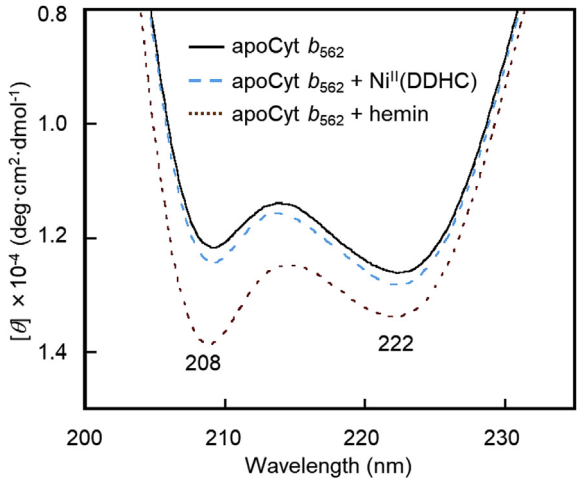

Fig. 6. CD spectral changes of apoCyt b_{562} upon addition of 5.0 eq of Ni^{II}(DDHC) (cyan broken line) or hemin (brown dotted line) in 100 mM potassium phosphate buffer (pH 7.0) at 25 °C. (For interpretation of the references to colour in this figure legend, the reader is referred to the Web version of this article.)

metal complexes into the binding pocket of the apo-form induces re-folding of the protein matrices with a stronger Cotton effect in the ultraviolet region [40,41]. However, the binding affinity of Ni^{II}(DDHC) to apoCyt b_{562} appears to be relatively low because the increase of CD spectral intensity in the ultraviolet region is less than the increase of CD spectral intensity caused by binding of hemin. Assuming complete refolding of the α-helices upon addition of the metal complex, 27% of Cyt b_{562} is reconstituted with Ni^{II}(DDHC) compared to Cyt b_{562} fully reconstituted with hemin, which is estimated by the intensity at 222 nm under conventional conditions. Furthermore, ESI-TOF MS gives a peak at $m/z = 2497.5$, which is consistent with the expected value of rCyt b_{562}(Ni^{II}(DDHC)) ($m/z = 2497.3$ ($z = 5+$)) (Fig. S5). The conjugation of Ni^{II}(TDHC) and apoCyt b_{562} also produces rCyt b_{562}(Ni^{II}(TDHC)), as confirmed by UV−vis and CD spectral changes (Figs. S6 and S7).

Methane generation from reconstituted Cyt b_{562} was then demonstrated in 100 mM potassium phosphate buffer (pH 7.0) at 25 °C under an N_2 atmosphere. First, we used dithionite or titanium(III) citrate to reduce Ni^{II}(DDHC) in the protein matrix, but methane generation was not observed. Therefore, we tried to reduce the Ni^{II}(DDHC) species with photoirradiation in the presence of tris(2,2′-bipyridine)ruthenium(II) chloride as a photosensitizer and sodium ascorbate as a sacrificial reagent. A solution of Ni^{II}(DDHC) or Ni^{II}(TDHC) (final conc.: 50 μM), apoCyt b_{562} (final conc.: 150 μM), tris(2,2′-bipyridine)ruthenium(II) chloride (final conc.: 100 μM) and sodium ascorbate (final conc.: 100 mM) dissolved in 100 mM potassium phosphate buffer (pH 7.0) (100 μL in total) was prepared. After 2 h of photoirradiation with a Xe-lamp, gaseous products were analyzed and quantified by gas chromatography (GC). The GC traces used to evaluate the amounts of methane are shown in Fig. 7 and the retention time of observed peaks for methane generated by the reconstituted proteins are consistent with the retention time of authentic methane gas. Other gaseous products such as ethane were not detected in this reaction. Fig. 8 summarizes the methane generation results produced by Ni^{II}(DDHC), the apoprotein and reconstituted Cyt b_{562} variants. Although control experiments with Ni^{II}(DDHC) itself or apoCyt b_{562} generated negligible amounts of methane, a small amount of methane (24 pmol, yield: 0.16% based on apoCyt b_{562} and turnover number (TON): 0.0049 based on Ni(TDHC)) was observed from rCyt b_{562}(Ni^{II}(TDHC)). Interestingly, a 12-fold greater amount of methane (290 pmol, yield: 1.9% base on apoCyt b_{562} and TON: 0.057 based on Ni(DDHC)) was generated from rCyt b_{562}(Ni^{II}(DDHC))

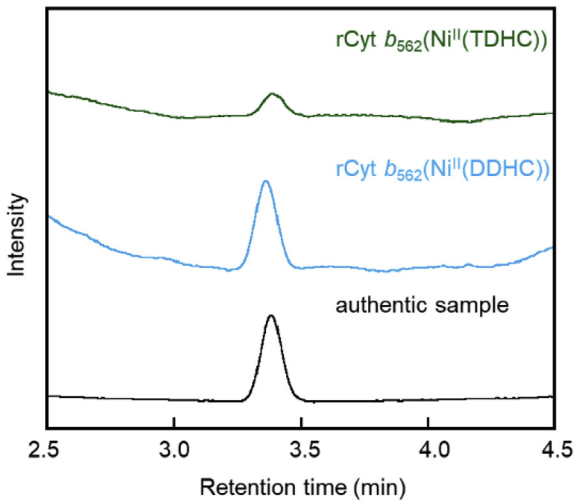

Fig. 7. GC traces of the reaction with rCyt b_{562}(Ni^{II}(TDHC)) (green line) and rCyt b_{562}(Ni^{II}(DDHC)) (cyan line) in the presence of tris(2,2′-bipyridine)ruthenium(II) chloride and sodium ascorbate in 100 mM potassium phosphate buffer (pH 7.0) at 25 °C under an N_2 atmosphere. Authentic methane gas is shown with a black line. (For interpretation of the references to colour in this figure legend, the reader is referred to the Web version of this article.)

relative to the amount of methane generated from rCyt b_{562}(Ni^{II}(TDHC)). The efficient methane generation from rCyt b_{562}(Ni^{II}(DDHC)) is likely due to the difference in the reactivity of the Ni(I) species as expected by the CV measurements. It is found that the redox potential of Ni^{II}(DDHC) is more negative than that of Ni^{II}(TDHC) in acetonitrile (Figs. 4 and S4) and the Ni(I) species of Ni(DDHC) shows high reactivity. Furthermore, the redox potential of rCyt b_{562}(Ni^{II}(DDHC)) in a buffer solution appears to be more negative than that of rCyt b_{562}(Ni^{II}(TDHC)), as seen in the more negative redox potential of Co(DDHC) relative to Co(TDHC)

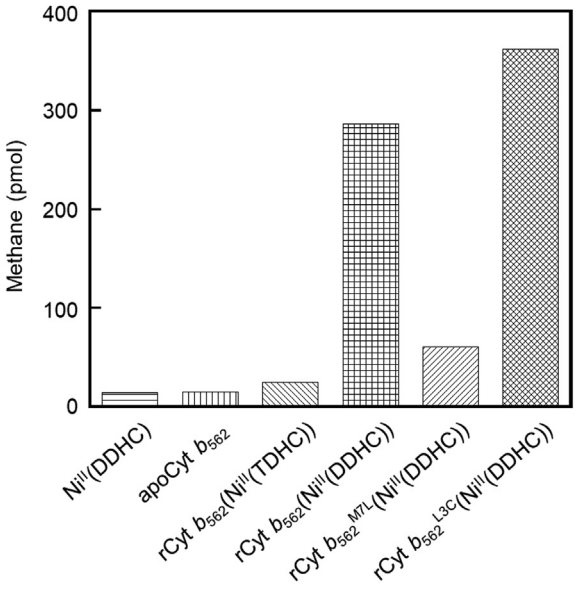

Fig. 8. Generated amounts of methane from Ni^{II}(DDHC), apoCyt b_{562}, rCyt b_{562}(Ni^{II}(TDHC)), rCyt b_{562}(Ni^{II}(DDHC)), rCyt b_{562}^{M7L}(Ni^{II}(DDHC)) and rCyt b_{562}^{L3C}(Ni^{II}(DDHC)) after 2 h of photoirradiation. Conditions: total volume 100 μL, [Ni^{II}(DDHC)] = 50 μM, [apoCyt b_{562} variant] = 150 μM, [[Ru(bpy)$_3$]Cl$_2$] = 100 μM, [sodium ascorbate] = 100 mM in 100 mM potassium phosphate buffer (pH 7.0) for 2 h at 25 °C under an N_2 atmosphere.

regardless of the presence and absence of the protein matrix [35].

In nature, cofactor and substrates are precisely located within the protein matrix [11,12,27,28]. According to the crystal structure of MCR, methyl-coenzyme M binds to the hydrophobic pocket above F430 with a predominant electrostatic interaction between the protein matrix and its sulfonate tail, indicating that the CH_3S group of methyl-coenzyme M is fixed close to and directed towards the cofactor [11,12,17,25]. On the other hand, the thiol group of coenzyme B is found to be placed at a proper distance from methyl-coenzyme M and F430 within the funnel-shaped channel of MCR. These suitable arrangements of substrates and active cofactor are essential to cleave the C–S bond and generate methane. Generally, the proximity effect promotes a reaction between an amino acid residue and an active cofactor in the protein matrix. For example, Watanabe and co-workers reported the hydroxylation of the Trp43 residue which is close to high-valent iron(IV)–oxo complex of heme within the binding pocket of the F43W/H64L mutant of myoglobin [42,43]. We also reported transmethylation from methylated Co(TDHC) to His64 which is located close to the cofactor within myoglobin reconstituted with Co(TDHC) [44]. According to these examples, we propose that the Ni(I) species of Ni(DDHC) activates the CH_3S group of Met7 close to the metal center within the heme-binding pocket of Cyt b_{562} to produce methane in this study although the detailed reaction mechanism is currently under investigation. To confirm the possibility of the CH_3S group of Met7 as an intraprotein substrate, we conducted the same experiment with a mutated protein matrix, Cyt b_{562}^{M7L}, in which Met7 was replaced with Leu. The significant decrease of methane generation was demonstrated from rCyt b_{562}^{M7L}(Ni^{II}(DDHC)) (60 pmol, yield: 0.40% based on apoCyt b_{562}^{M7L} and TON: 0.012 based on Ni(DDHC)) (Fig. 8). This is caused by the protein matrix lacking a suitable intraprotein methyl donor, the CH_3S group of Met7, in the active site. To evaluate the demethylation of the protein matrices, mass spectral analysis was carried out after isolation and concentration of the protein matrices of rCyt b_{562}(Ni^{II}(DDHC)) and rCyt b_{562}^{M7L}(Ni^{II}(DDHC)). The ESI-TOF mass spectrum of rCyt b_{562}(Ni^{II}(DDHC)) after the reaction has characteristic peaks at m/z = 1964.42 (z = 6+) and 1961.59 (z = 6+) as shown in Fig. 9a. The former peak is assigned to the protein matrix of apoCyt b_{562} (calcd.: m/z = 1964.18 (z = 6+)), whereas the latter is consistent with the calculated m/z for demethylated apoCyt b_{562} where one methyl group is absent from the protein matrix (calcd.: m/z = 1961.84 (z = 6+)). In contrast, the ESI-TOF mass spectrum of rCyt b_{562}^{M7L}(Ni^{II}(DDHC)) after the reaction has a single peak at m/z = 1961.34 (z = 6+) as shown in Fig. 9b. This peak is attributed to the protein matrix of apoCyt b_{562}^{M7L} (calcd.: m/z = 1961.18 (z = 6+)) suggesting that the demethylation of any residues in rCyt b_{562}^{M7L}(Ni^{II}(DDHC)) is ruled out. Thus, the protein matrix of rCyt b_{562}^{M7L}(Ni^{II}(DDHC)) retains its molecular weight during the reaction. The present findings suggest that methane is clearly derived from Met7 via C–S bond cleavage by the active Ni^{I}(DDHC).

Cyt b_{562}^{L3C}, a Cyt b_{562} mutant in which Leu3 is replaced with Cys, was also prepared in order to provide and fix a thiol group mimicking another native substrate, coenzyme B, close to the reaction center (Fig. 2a). Interestingly, the Cys3 residue clearly increases the amount of methane gas generation (360 pmol, yield: 2.4% based on apoCyt b_{562}^{L3C} and TON: 0.072 based on Ni(DDHC)) by 24% compared to rCyt b_{562}(Ni^{II}(DDHC)) as shown in Fig. 8. This finding suggests that the thiol group of Cys3 contributes to a hydrogen transfer to produce methane as seen in the thiol group of coenzyme B in the reaction scaffold of MCR.

4. Conclusion

Ni^{II}(DDHC) is an appropriate model complex of F430 compared

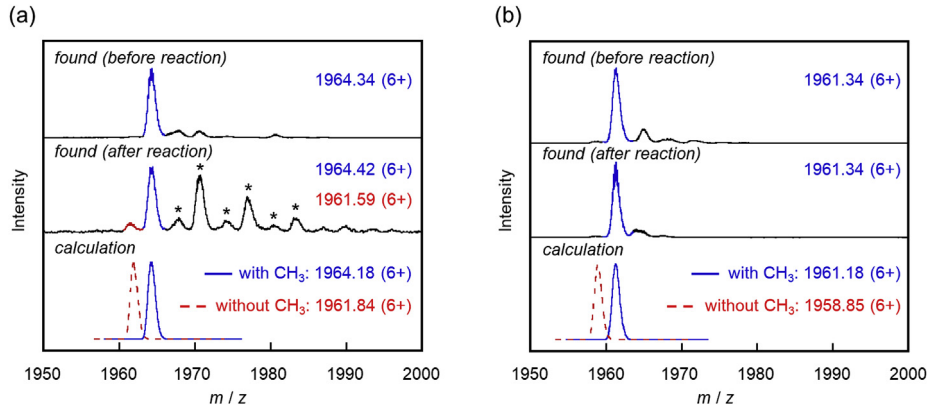

Fig. 9. ESI-TOF mass spectra of protein matrices of (a) rCyt b_{562}(N^{II}(DDHC)) and (b) rCyt $b_{562}{}^{M7L}$(N^{II}(DDHC)). Upper and middle spectra show the results obtained before and after the reaction, respectively. Bottom profiles represent the calculated spectra showing protein matrices retaining the CH_3 group (blue solid line) and losing one CH_3 group (red broken line). The asterisks in (a) and (b) indicate potassium and sodium adducts of the protein matrices, respectively. (For interpretation of the references to colour in this figure legend, the reader is referred to the Web version of this article.)

to Ni^{II}(TDHC), because the more negative Ni^{II}/Ni^{I} redox potential of Ni(DDHC) is expected to provide a highly reactive Ni(I) species compared to that of Ni(TDHC). Therefore, in the present investigation, it was possible to detect methane generation initiated by Ni(DDHC) in the Cyt b_{562} matrix which has a thioether group derived from the methionine residue in the cofactor binding cavity. Photoirradiation of rCyt b_{562}(Ni^{II}(DDHC)) in the presence of a photosensitizer and a sacrificial reagent resulted in efficient methane generation. Furthermore, comparison of the results of methane generation and mass changes of protein matrices between rCyt b_{562}(Ni^{II}(DDHC)) and rCyt $b_{562}{}^{M7L}$(Ni^{II}(DDHC)) provides evidence that methane is derived from the CH_3S group of Met7 via C—S bond cleavage by the reactive Ni(I) species in the protein matrix. In addition, the generation of methane gas from rCyt $b_{562}{}^{L3C}$(Ni^{II}(DDHC)) is found to be enhanced relative to methane generated from rCyt b_{562}(Ni^{II}(DDHC)). These results clearly indicate that precise arrangements of the thioether, the thiol and the nickel center provide efficient methane generation via cleavage of the C—S bond in the protein matrix. Therefore, methane generation by the reconstituted protein is promoted not only by having an appropriate nickel complex but also by the precise positions of thiol and thioether moieties in the 2nd coordination sphere. Two key residues, Met7 and Cys3, are regarded as substrate models of methyl-coenzyme M and coenzyme B, respectively. To the best of our knowledge, this study is the first example of methane generation via intraprotein cleavage of the C—S bond using a protein-based functional model of MCR. Further studies on methane generation via cleavage of a C—S bond within a protein matrix will contribute to the elucidation of the reaction mechanism of MCR as well as the development of artificial metalloenzymes inspired by MCR.

Conflicts of interest

The authors declare that there is no conflict of interest in publishing this paper.

Acknowledgements

This work was financially supported by Grants-in-Aid for Scientific Research provided by JSPS KAKENHI Grant Numbers JP15H05804, JP16H06045, JP17J00008, JP18KK0156, and JP18K19099. We appreciate support from JST PRESTO (JPMJPR15S2) and SICORP. Y.M. appreciates support from the JSPS Research Fellowship for Young Scientists.

Appendix A. Supplementary data

Supplementary data to this article can be found online at https://doi.org/10.1016/j.jorganchem.2019.120945.

References

[1] P.N. Evans, J.A. Boyd, A.O. Leu, B.J. Woodcroft, D.H. Parks, P. Hugenholtz, G.W. Tyson, Nat. Rev. Microbiol. 17 (2019) 219–232.
[2] G. Borrel, P.S. Adam, L.J. McKay, L.-X. Chen, I.N. Sierra-García, C.M.K. Sieber, Q. Letourneur, A. Ghozlane, G.L. Andersen, W.-J. Li, S.J. Hallam, G. Muyzer, V.M. Oliveira, W.P. Inskeep, J.F. Banfield, S. Gribaldo, Nat. Microbiol. 4 (2019) 603–613.
[3] B.C. McBride, R.S. Wolfe, Biochemistry 10 (1971) 2317–2324.
[4] D. Ankel-Fuchs, R.K. Thauer, Eur. J. Biochem. 156 (1986) 171–177.
[5] R.K. Thauer, Biochemistry (2019), https://doi.org/10.1021/acs.biochem.9b00164 in press.
[6] B. Jaun, A. Pfaltz, J. Chem. Soc., Chem. Commun. (1986) 1327–1329.
[7] B. Jaun, Helv. Chim. Acta 73 (1990) 2209–2217.
[8] R. Piskorski, B. Jaun, J. Am. Chem. Soc. 125 (2003) 13120–13125.
[9] B. Jaun, A. Pfaltz, J. Chem. Soc., Chem. Commun. (1988) 293–294.
[10] S.-K. Lin, B. Jaun, Helv. Chim. Acta 74 (1991) 1725–1738.
[11] U. Ermler, W. Grabarse, S. Shima, M. Goubeaud, R.K. Thauer, Science 278 (1997) 1457–1462.
[12] W. Grabarse, F. Mahlert, E.C. Duin, M. Goubeaud, S. Shima, R.K. Thauer, V. Lamzin, U. Ermler, J. Mol. Biol. 309 (2001) 315–330.
[13] M. Dey, R.C. Kunz, D.M. Lyons, S.W. Ragsdale, Biochemistry 46 (2007) 11969–11978.
[14] M. Dey, J. Telser, R.C. Kunz, N.S. Lees, S.W. Ragsdale, B.M. Hoffman, J. Am. Chem. Soc. 129 (2007) 11030–11032.
[15] N. Yang, M. Reiher, M. Wang, J. Harmer, E.C. Duin, J. Am. Chem. Soc. 129 (2007) 11028–11029.
[16] R. Sarangi, M. Dey, S.W. Ragsdale, Biochemistry 48 (2009) 3146–3156.
[17] P.E. Cedervall, M. Dey, X. Li, R. Sarangi, B. Hedman, S.W. Ragsdale, C.M. Wilmot, J. Am. Chem. Soc. 133 (2011) 5626–5628.
[18] V. Pelmenschikov, M.R.A. Blomberg, P.E.M. Siegbahn, R.H. Crabtree, J. Am. Chem. Soc. 124 (2002) 4039–4049.
[19] V. Pelmenschikov, P.E.M. Siegbahn, J. Biol. Inorg. Chem. 8 (2003) 653–662.
[20] S.-L. Chen, M.R.A. Blomberg, P.E.M. Siegbahn, Chem. Eur J. 18 (2012) 6309–6315.
[21] S.-L. Chen, M.R.A. Blomberg, P.E.M. Siegbahn, Phys. Chem. Chem. Phys. 16 (2014) 14029–14035.
[22] T. Wongnate, D. Sliwa, B. Ginovska, D. Smith, M.W. Wolf, N. Lehnert, S. Raugei, S.W. Ragsdale, Science 352 (2016) 953–958.
[23] M. Krüger, A. Meyerdierks, F.O. Glöckner, R. Amann, F. Widdel, M. Kube, R. Reinhardt, J. Kahnt, R. Böcher, R.K. Thauer, S. Shima, Nature 426 (2003) 878–881.
[24] S. Scheller, M. Goenrich, R. Boecher, R.K. Thauer, B. Jaun, Nature 465 (2010) 606–608.
[25] S. Shima, M. Krueger, T. Weinert, U. Demmer, J. Kahnt, R.K. Thauer, U. Ermler, Nature 481 (2012) 98–101.
[26] P.E. Cedervall, M. Dey, A.R. Pearson, S.W. Ragsdale, C.M. Wilmot, Biochemistry 49 (2010) 7683–7693.
[27] S. Ebner, B. Jaun, M. Goenrich, R.K. Thauer, J. Harmer, J. Am. Chem. Soc. 132 (2010) 567–575.
[28] M.W. Renner, L.R. Furenlid, K.M. Barkigia, A. Forman, H.K. Shim, D.J. Simpson,

K.M. Smith, J. Fajer, J. Am. Chem. Soc. 113 (1991) 6891–6898.
[29] G.K. Lahiri, L.J. Schussel, A.M. Stolzenberg, Inorg. Chem. 31 (1992) 4991–5000.
[30] L. Signor, C. Knuppe, R. Hug, B. Schweizer, A. Pfaltz, B. Jaun, Chem. Eur J. 6 (2000) 3508–3516.
[31] J. Nishigaki, T. Matsumoto, K. Tatsumi, Inorg. Chem. 51 (2012) 5173–5187.
[32] C. Brenig, L. Prieto, R. Oetterli, F. Zelder, Angew. Chem. Int. Ed. 57 (2018) 16308–16312.
[33] K. Oohora, Y. Miyazaki, T. Hayashi, Angew. Chem. Int. Ed. (2019), https://doi.org/10.1002/anie.201907584 in press.
[34] Y. Murakami, Y. Aoyama, K. Tokunaga, J. Am. Chem. Soc. 102 (1980) 6736–6744.
[35] Y. Morita, K. Oohora, A. Sawada, T. Kamachi, K. Yoshizawa, T. Hayashi, Inorg. Chem. 56 (2017) 1950–1955.
[36] F.W.J. Teale, Biochim. Biophys. Acta 35 (1959) 543.
[37] C.-A. Yu, I.C. Gunsalus, J. Biol. Chem. 249 (1974) 107–110.
[38] H. Kitagishi, K. Oohora, H. Yamaguchi, H. Sato, T. Matsuo, A. Harada, T. Hayashi, J. Am. Chem. Soc. 129 (2007) 10326–10327.
[39] F.S. Mathews, P.H. Bethge, E.W. Czerwinski, J. Biol. Chem. 254 (1979) 1699–1706.
[40] T. Hayashi, Y. Morita, E. Mizohata, K. Oohora, J. Ohbayashi, T. Inoue, Y. Hisaeda, Chem. Commun. 50 (2014) 12560–12563.
[41] K. Oohora, T. Hayashi, Methods Enzymol. 580 (2016) 439–454.
[42] I. Hara, T. Ueno, S. Ozaki, S. Itoh, K. Lee, N. Ueyama, Y. Watanabe, J. Biol. Chem. 276 (2001) 36067–36070.
[43] T.D. Pfister, T. Ohki, T. Ueno, I. Hara, S. Adachi, Y. Makino, N. Ueyama, Y. Lu, Y. Watanabe, J. Biol. Chem. 280 (2005) 12858–12866.
[44] Y. Morita, K. Oohora, A. Sawada, K. Doitomi, J. Ohbayashi, T. Kamachi, K. Yoshizawa, Y. Hisaeda, T. Hayashi, Dalton Trans. 45 (2016) 3277–3284.